The International Journal of Advanced Manufacturing Technology (2019) 104:3327–3333
https://doi.org/10.1007/s00170-018-2596-3

ORIGINAL ARTICLE

Fabrication and characterization of gold-coated solid silicon microneedles with improved biocompatibility

S. Pradeep Narayanan[1] · S. Raghavan[2]

Received: 21 February 2017 / Accepted: 15 August 2018 / Published online: 17 September 2018

Abstract

In this paper, we discussed biocompatibility improvement and mechanical strength of the solid silicon (Si) microneedles for transdermal drug delivery systems. The pyramidal shape and sharp tip of microneedles are fabricated using an optimized Tetramethylammonium Hydroxide (TMAH) etching factors. The mechanical strength and biocompatibility of the microneedle array are enhanced after coating gold (Au) layer through metal sputtering technique. The needles thus fabricated are suitable for sustained transdermal drug delivery applications with a height of 250 μm and a base width of 52.8 μm, the aspect ratio of 4.73, and tip angle and diameter of 24.5° and 45 μm. The Vickers hardness value of 3800 Hv is obtained for the fabricated Au-coated solid Si microneedles. The attained Vickers hardness value is substantially higher than the skin resistive force. It shows that the capability of drug delivery by piercing these microneedles into the skin becomes readily feasible.

Keywords Biocompatibility · Hardness · Metal sputtering · Microneedles · Transdermal drug delivery

1 Introduction

Development of drug delivery techniques occurred after using transdermal systems for applications. Transdermal systems are less expensive, non-invasive and control drug release, all of which develop patient's conformity to real-time usage [1]. Though other transdermal system methods vary in mechanisms and principles, the aim is to improve drug absorption while crossing the Stratum Corneum (SC) layer of the skin. It is achieved either by creating pores or developing the dispersed contacts [1, 2]. Among most of the physical methodologies, microneedles achieved success rapidly when compared to other devices. It acts as transdermal patches during drug delivery applications with a promising and an adequate method of increasing drug permeability delivery via the skin [3, 4]. They assist drug molecule movements in blood flow while delivering vaccines into the skin or dendritic cells [5, 6]. Microneedles made using silicon (Si) as a base enhanced the pharmaceutical contributions, especially towards drug metabolization. In the last two decades, microneedles role as a pain-free system in transdermal drug delivery systems increased. It became possible due to reducing or avoiding nerve stimulus pain. Even now, silicon-based microneedles are improving because of their promptness to be incorporated into other devices like silicon-based BioMEMS sensors, actuators, etc.

Various manufacturing techniques were summarized in the variation of shape and size of microneedles for transdermal drug delivery applications [7]. Of them, usage of solid and hollow microneedles was reviewed broadly [8–15]. Drug delivery into the body through hollow microneedles needs external support like micropump or a syringe. So this type of microneedle is highly suitable for sustained drug deliveries. However, when using solid microneedles, drugs could be delivered in the form of a transdermal patch or else drug release from the tips by poking the skin. Later, a familiar method was to coat the drugs at microneedles tip and deliver it into the skin. The drugs diffuse this way adequately by separating from the microneedle array thereby attaining more potency

✉ S. Pradeep Narayanan
narenpradeep@gmail.com

[1] Department of Electronics and Communication Engineering, Kalasalingam Academy of Research and Education, Krishnan Kovil, Tamil Nadu, India

[2] Department of Electronics and Communication Engineering, National Institute of Technology, Tiruchirappalli, Tamil Nadu, India

[16, 17]. All categories of solid microneedles should have higher biocompatibility to cross the SC layer of the skin during drug delivery.

Though silicon-integrated MEMS technology influenced transdermal drug delivery, it is not biocompatible as an implantable device. Vast research on microneedles was carried out on microfluidic transdermal applications where it transfers almost all liquid form of drugs [18, 19]. Improving biocompatibility of the microneedles becomes mandatory, both for specific drug dosing and skin penetration. Rapid technologies are incorporated to recognize biocompatibility in microneedles either using metals, polymers, ceramics (glass), etc. Still, extensive research is needed in metals, polymers, and ceramics to produce in large numbers.

The optimization and analyses were reported in our other study [17]. With the optimized parameters, our aim is to enhance the mechanical strength and biocompatibility of the solid Si microneedles by inducing metal deposition on it. In this work, we described the design, fabrication, and characterization of the high aspect ratio of solid Si microneedles using a two-step process of combining lithography with anisotropic wet etching (TMAH) process. Metal deposition is made through a sputtering technique to make the fabricated microneedles more biocompatible. Chromium as a seed layer and gold as a metal layer is chosen. The mechanical ability and its strength are tested by the Vickers hardness testing tools. The results described indicate a broad opening in biocompatible transdermal drug delivery devices.

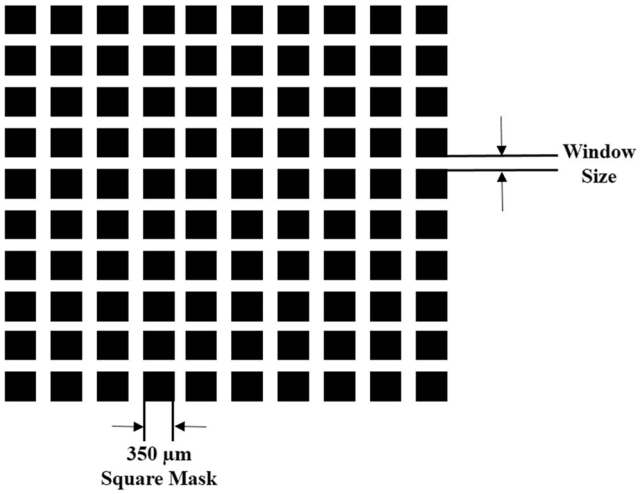

Fig. 1 Mask design for gold-coated solid Si microneedles

2 Experiment

2.1 Fabrication of solid Si microneedles

Fabrication was made with the optimized parameters, to ensure the high aspect ratio and improve the biocompatibility of solid Si microneedles. Figure 1 shows the optical mask size used, with a unique spacing of 500 µm on all sides. Double Side Polished (DSP) 525 µm thickness silicon wafer of P-type with [1 0 0] orientation and a resistivity of 4-7 ohm/cm was used for fabrication. Radio Corporation of America (RCA) cleaning was made on the wafer first for 30 min to remove impurities and then dried by blowing nitrogen. The cleaned Si wafer was predeposited by the oxide layer using wet oxidation furnace. The wafer was then coated with S1813 (Microfabrication Materials Technologies, Austin, TX) photoresist and spun for 30 s at 3000 RPM with a prespin of 15 s at 300 RPM, then prebaked at 90 °C for 120 s. It achieved the Positive Photoresist (PPR) thickness of 2 µm and the wafer was then aligned with the chosen optical mask. Ultraviolet rays were exposed on the wafer using a Karl Suss MJB4 mask aligner, developed and hard baked later for 120 s at 90 °C. In other steps, unprotected silicon dioxide (SiO_2) and photoresist layers were removed using their etchants. TMAH etching was carried over the Si wafer with the optimized 1:8:1 (TMAH:Deionized (DI) Water:Isopropyl Alcohol (IPA)) concentration. Back oxide layer limits etching to the exposed area, by preventing the Si wafer from any damage. On regular intervals, Si microneedles were monitored and shown clearly in Figs. 4 and 5. Finally, an array of high aspect ratio solid Si microneedles with a height of 250 µm and a base width of 52.8 µm, aspect ratio of 4.73, and tip angle and diameter of 24.5° and 45 µm was obtained as shown in Fig. 6.

2.2 Metal deposition on solid Si microneedles

The step by step process used to fabricate metal-coated solid Si microneedles was examined precisely in Fig. 2. To make them fit for transdermal drug delivery and to improve their biocompatibility, a gold (Au) metal layer was coated on the fabricated solid Si microneedles. Chromium (Cr) metal was deposited as a seed layer of 200 nm over the Si microneedles using metal-sputter system (Nordiko Technical Services Ltd., Hampshire, UK) as shown in Fig. 7a. For proper conduction of Au layer, the Cr seed layer is mandatory. Then, 1000 nm of Au was coated on the Cr-coated Si microneedles using the same metal sputtering technique. Both the coatings were made one by one by keeping the Si wafer in a vacuum within the sputtering system. After the final deposition of the metal layer over the solid Si microneedles, the presence of metal elements including Cr was observed from the Energy Dispersive X-ray spectroscopy (EDX) spectrum as shown in Fig. 7b. The spectrum exhibits 70% weight of Au, 2% weight of Cr, 25% weight of Si, 2% weight of O (oxygen), and 1% weight of C (carbon).

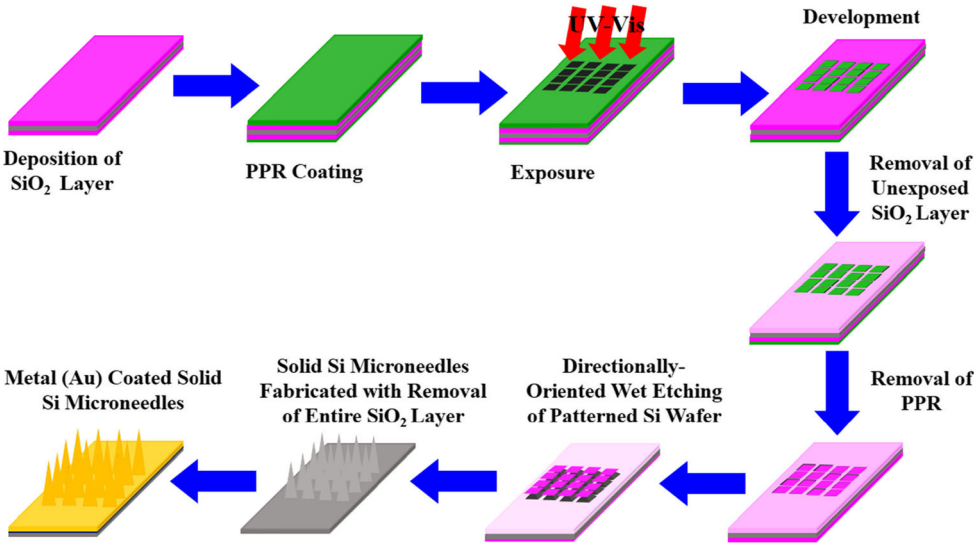

Fig. 2 3D process flow of making gold-coated solid Si microneedle array

2.3 Mechanical testing

An experiment of hardness calculation was made using Vickers hardness test to determine the ultimate breaking value of microneedles for the applied force. It gives the mechanical strength of microneedles that helps, whereas penetrating into the skin. All the samples kept one by one within the holder to check and compare its withstand values. The load of 10 gram force (gf) was initiated and varied slowly up to 180 gf in the addition of each 10 gf for every test made. The indenter tip will hit the samples with a dwell time of 20 s, for which the obtained values were recorded and plotted as a graph shows the variations of applied force versus hardness value (Hv) as shown in Fig. 8.

3 Results and discussion

3.1 Profilometer and ellipsometer analysis

The thickness of SiO_2 layer grown over a cleaned Si wafer using the wet thermal oxidation method is measured using Sentech ellipsometer (SE 800 model) by passing light rays over the wafer kept on the holder, after fixing it at a particular angle of 70°. We measured five different spots on the wafer to make sure that the oxide layer grew uniformly. The measured results are shown in Fig. 3. It gives a thickness of 1 μm, comparatively.

PPR S1813 is spin coated over the SiO_2 layer grown Si wafer which transfers the pattern from mask to the wafer while doing photolithography. Ambios XP-2 surface profilometer is used to measure the thickness of the coated PPR with its step height marked in five different regions. Hence, a thickness of 2 μm is perceived for PPR and shown in Fig. 3.

3.2 Field emission scanning electron microscope results

TMAH etching with an optimized concentration of 1:8:1 (TMAH:DI:IPA) solution is carried over the patterned (lithographed) Si wafer. The etched Si wafer is observed after 30 min once the etching begins. 1 cm × 1 cm Si microneedles are kept on the sample holder for imaging, and the hexagonal shape formed as its base is shown in Fig. 4.a, b. It confirms uniform etching without any disturbances. Si microneedles examined in a different area (2 × 2 array) show no damages, as spotted in Fig. 4c. All the images are observed using Field Emission Scanning Electron Microscope (FESEM). Figure 4d is the proof of the unique shape and smooth etching profile developed on the patterned Si wafer to form solid Si microneedles.

Figure 5a, b shows that controlled etching is undertaken to induce solid Si microneedles. Still, a protective SiO_2 layer present on the Si microneedles starts growing after etching for 1 h and 1.5 h, respectively. It initiated a pyramid-like structure with

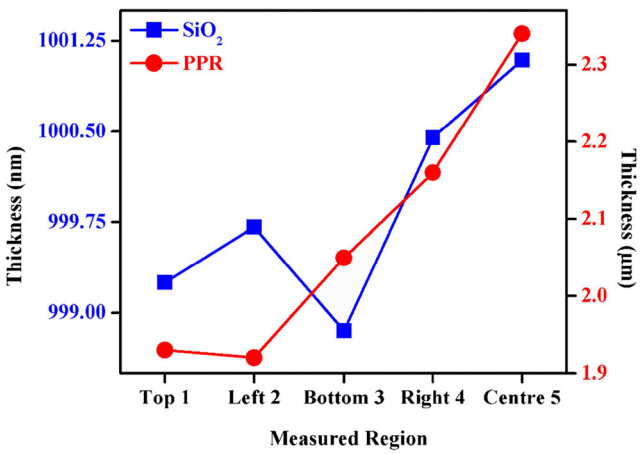

Fig. 3 Thickness measurements of SiO_2 and PPR S1813

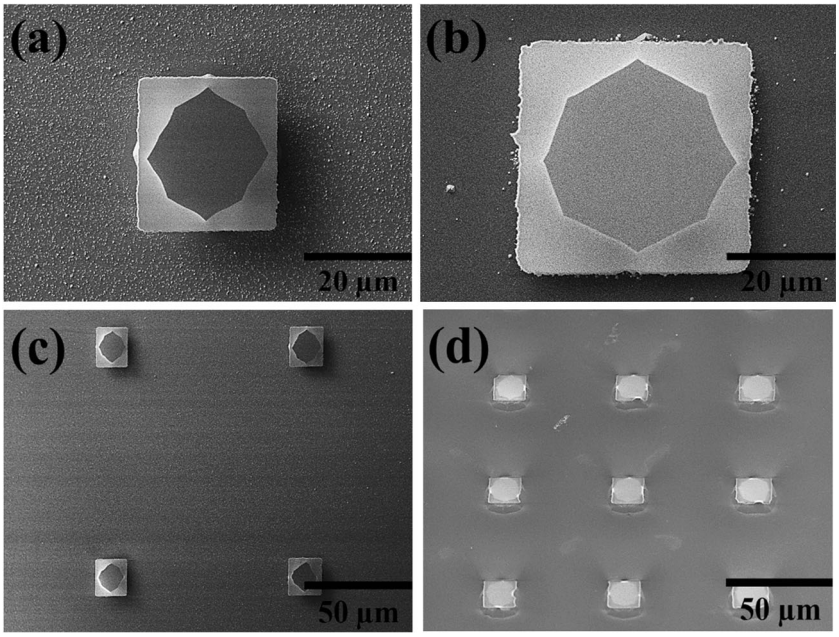

Fig. 4 **a**, **b** Hexagonal shape base of single microneedle in different areas (shows that etching was initiated smoothly). **c** 2 × 2 array of solid Si microneedle with center to center spacing of 500 µm. **d** 3 × 3 array of microneedle with smooth surface

a hexagonal base. The surface morphology of the etched Si microneedles as determined in Fig. 5c shows that it has a smooth etched surface with a partial protective layer. The morphology of the Si microneedles formed to the desired shape of the patterned Si wafer is shown in Fig. 5d. The surface profile becomes smoother after increasing etching time at regular intervals.

Though etching time was already optimized by us [17], we find the growth of Si microneedles through 2.5 h, where a whole process is carried out. It provided a path to etch more till it reaches the desired pyramidal shape of Si microneedles with sharp tips. Uniformity of etching is seen over the entire patterned Si wafer. Getting a high aspect ratio for solid Si microneedles is mandatory. The protective SiO_2 layer peels off from the formed Si microneedles is shown in Fig. 6a. Interestingly, Fig. 6b shows an array of solid Si microneedle fabricated successfully with a height of 250 µm. Its base width is 52.8 µm, aspect ratio 4.73, tip angle 12.5°, and tip diameter of 45 µm.

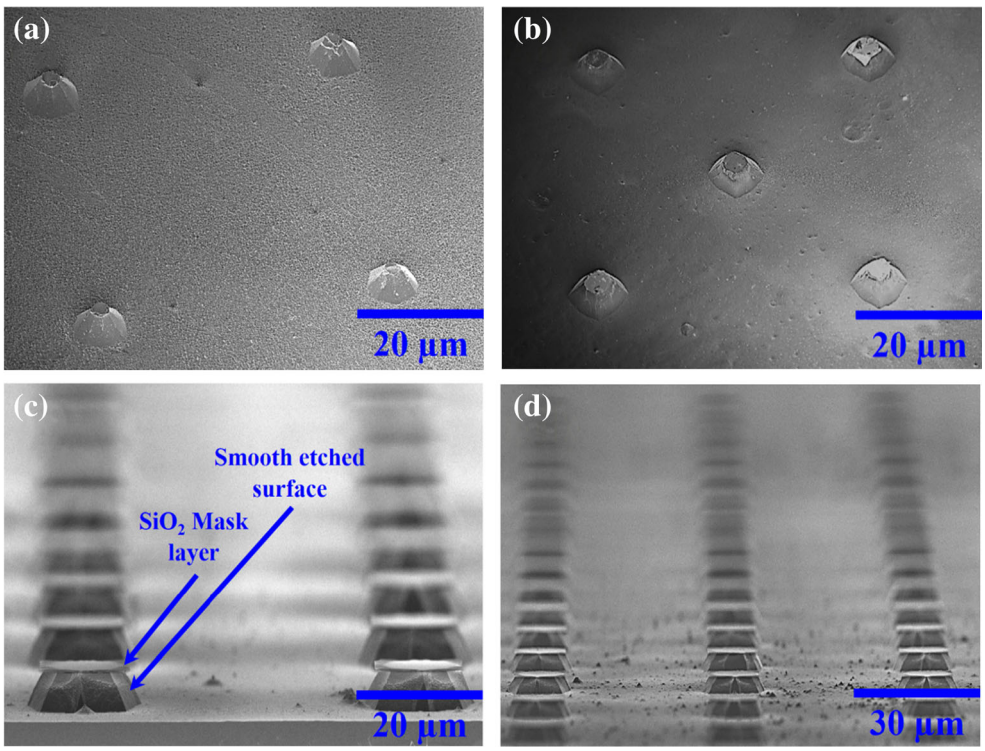

Fig. 5 **a** After 1 h of etching (2 × 2 array of microneedle). **b** 1.5 h of etching (microneedles). **c** 2 h of etching (2 rows of microneedles). **d** Group of microneedles after 2.5 h of etching

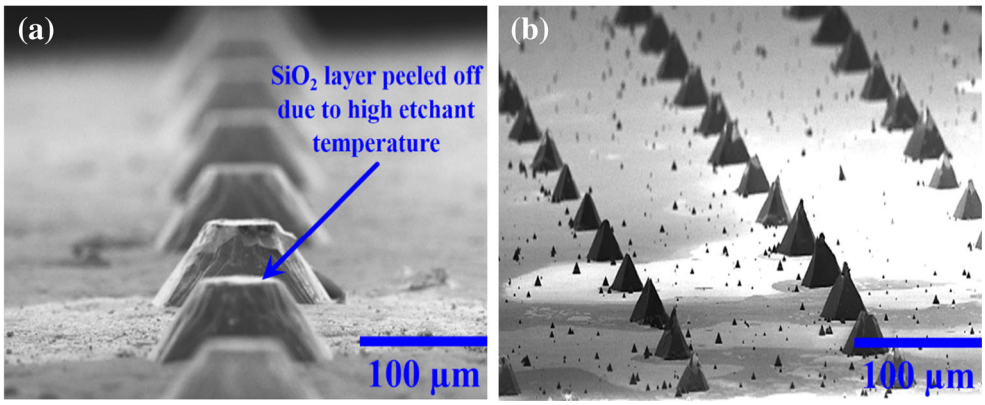

Fig. 6 **a** Single row of microneedles with the SiO_2 layer peeled off. **b** Final high aspect ratio of solid Si microneedles

After observing the high aspect ratio of solid Si microneedles, we improved its biocompatibility by coating metal on their tips. Fabrication of the metal-coated Si microneedles is always easy using micromachining technique compared to conventional micromachining techniques. The metal deposition is made on Si microneedles to make them appropriate biocompatible devices and increase its mechanical strength to penetrate the skin for drug delivery without causing side effects and damage. For this study, fabricated sharp, high aspect ratio solid Si microneedles are kept over the target of the metal sputtering system under vacuum, where metal atoms are ejected from the target and bombarded on the microneedles. To sputter gold as a metal layer (1000 nm), chromium is first coated as a seed layer (200 nm) to improve adhesion between microneedles and metal deposition. Finally, the fabricated Au-coated solid Si microneedles are shown along with its EDX spectrum in Fig. 7a, b. The EDX spectrum confirms the presence of metals absorbed in the fabricated microneedles. To have contact with the skin to deliver drugs, only the coated Au will have a bond, not Si. It makes coated Si microneedles suitable as a biocompatible device for drug delivery. Here, the entire images are captured using Zeiss Ultra 55 FESEM with Oxford EDX system with a higher resolution of 1.2 nm @ 15 KV. Acceleration voltage (Vacc) used here is 5 KV and the sample holder is tilted up to 45° angle to examine the growth in exact size, i.e., microneedle height.

3.3 Mechanical strength test analysis

Microneedles are tested for their ultimate breaking strength through a load versus Vickers hardness (Hv) variation, noted from the bare Si wafer to the finally obtained metal-coated Si microneedle array (layer by layer). Applied load (L) is varied in 10 gf for all the used samples, till it is broken, indicating the maximum weight it withstands. Comparison of load variations and the ultimate hardness value is observed and shown in Fig. 8. Among them, only gold-coated Si microneedles withstand a maximum load of up to 180 gf. If the applied load goes above 180 gf, microneedles are broken, and the hardness value comes down from its ultimate point. We eventually determined that the Vickers hardness value is nearly 3800 Hv for the fabricated and tested microneedles. The converted pressure value is close to 37.27 GPa.

We considered all hardness values cumulatively for 150 gf of the applied load, as coated Si microneedles withstand up to 180 gf. As a result, after 150 gf all the other comparative devices like bare Si wafer, SiO_2 layer coated Si wafer, PPR coated on Si wafer and obtained Si microneedles gets break. The obtained results are illustrated in Fig. 9. The coated Si microneedles provide the pressure of 30.4 GPa approximately at 150 gf. If the area of tips is reduced, it decreases the insertion force of microneedles as reported [20, 21]. Some works in

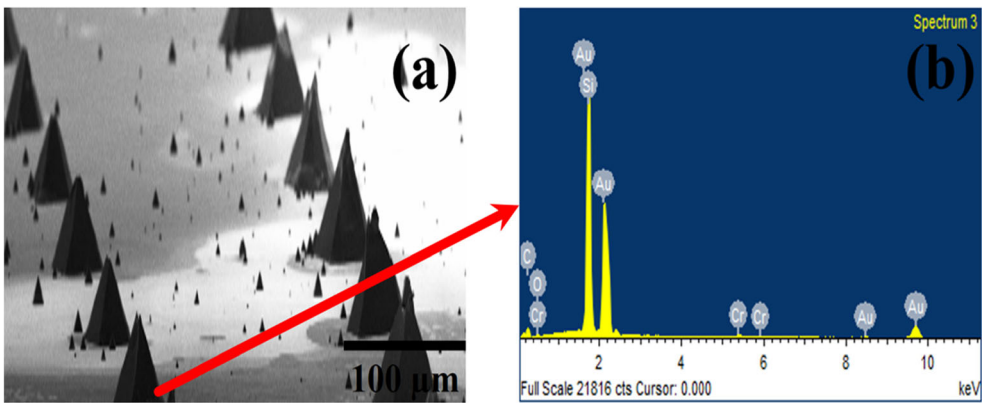

Fig. 7 **a** An array of Au-coated solid Si microneedle (finally fabricated). **b** EDX spectrum of Au-coated solid Si microneedles

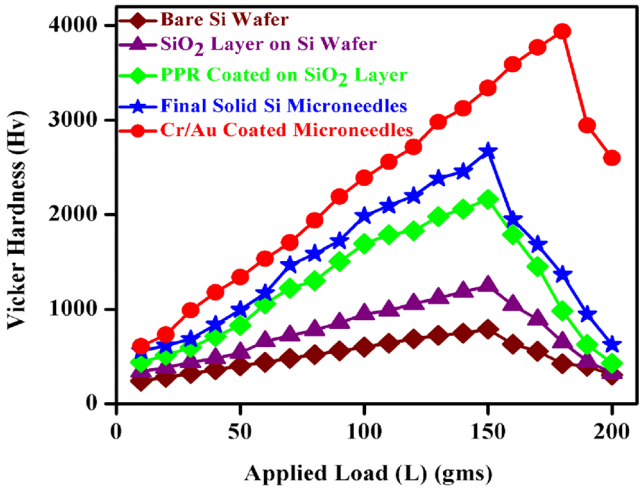

Fig. 8 Measured and compared—load versus Vickers hardness (Hv) values for all samples

literature have shown that the sharpness of microneedles tips will increase skin permeability while penetrating the skin [22, 23]. Fabricated microneedles provide a pressure of nearly 30 GPa, which is higher than the resistive force of the skin, i.e., 3.18 MPa. Thus, the obtained result shows that fabricated Si microneedles suits perfectly for insertion of drugs through the skin with no damage.

A cross section of human skin along with inserted gold-coated solid Si microneedles is shown in Fig. 10, while it is seen that the outermost SC layer thickness is 10–40 μm. Consequently, it has two more layers named epidermis with a thickness of 50–150 μm and dermis with 500–1500 μm. Inflict restrictions from the skin layers are to be counted while designing microneedles with proper length to deliver drugs efficiently. It is clear that to have a pain-free and impermeable transdermal drug delivery, microneedles length should penetrate more than 150 μm into the skin [17, 24].

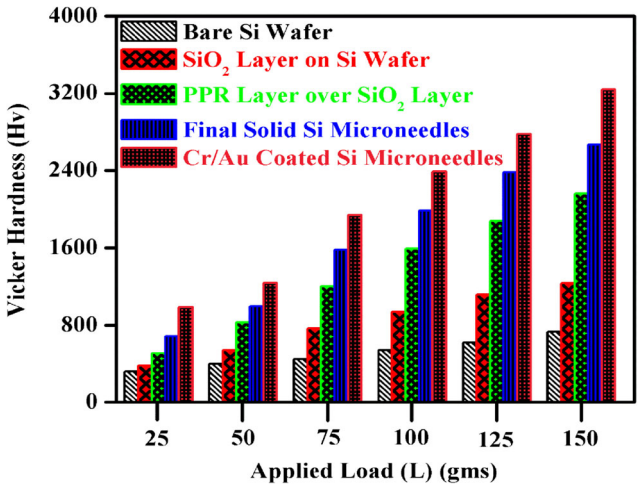

Fig. 9 Cumulative value of 150 gf is taken and compared (fabricated Au-coated solid Si microneedles with other samples)

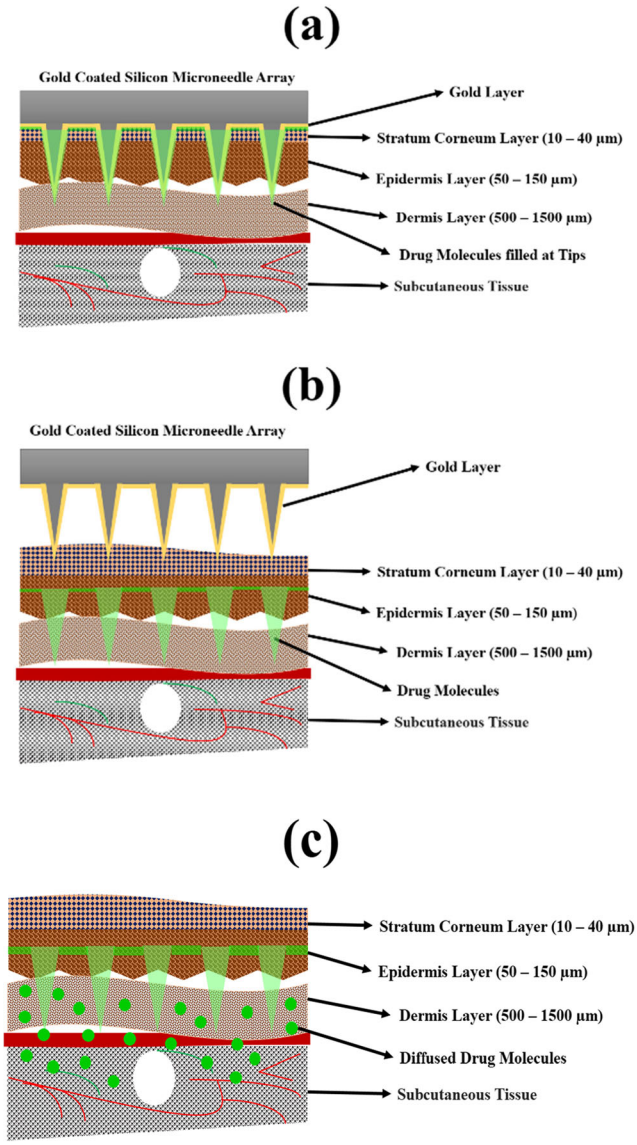

Fig. 10 Cross section of human skin implanted with gold-coated solid Si microneedles with **a** Drug molecules at its tips, **b** Removal of microneedles after drug release, and **c** Diffused drug molecules into the skin

4 Conclusion

A simple and cost-effective process for fabricating solid Si microneedles with a high aspect ratio is evaluated by us using single step optimized anisotropic TMAH etching. To improve the solid Si microneedles biocompatibility a metal (Au) layer is coated on it. The mechanical strength of fabricated microneedles is calculated from the Vickers hardness test. It is observed that microneedles, can penetrate the skin without any fractures due to its higher-pressure value than the skin's resistive force. Thus, biocompatibility of microneedles improved more after it is metal coated, where gold is having very good adhesive properties and calculated mechanical strength in hardness value as 37.27 GPa. With all the acquired parameters, it is seen that this

microneedle opens a broad way of research in the applications of biocompatible drug delivery devices in transdermal systems.

Acknowledgements The authors gratefully acknowledge the support provided by the Indian Nanoelectronics Users Programme (INUP)—IIT Bombay (IITB), India, to carry out this work and also to CEN (Centre of Excellence in Nano Technology), IITB, for their permission to use the available facilities.

References

1. Prausnitz MR (2004) Microneedles for transdermal drug delivery. Adv Drug Deliv Rev 56:581–587
2. Prausnitz MR, Langer R (2008) Transdermal drug delivery. Nat Biotechnol 27:1261–1268
3. Kaestli LZ, Wasilewski-Rasca AF, Bonnabry P, Vogt-Ferrier N (2008) Use of transdermal drug formulations in the elderly. Drugs Aging 25:269–280
4. Sivamani RK, Liepmann D, Malbach HI (2007) Microneedles and transdermal applications. Expert Opin Drug Deliv 4:19–25
5. Kalluri H, Banga AK (2011) Transdermal delivery of proteins. AAPS PharmSciTech 12:431–441
6. Hadgraft J, Lane ME (2011) Skin: the ultimate interface. Phys Chem Chem Phys 13:5215–5222
7. Xiang Z, Wang H, Pant A, Pastorin G, Lee C (2013) Development of vertical SU-8 microtubes integrated with dissolvable tips for transdermal drug delivery. Biomicrofluidics 7(2):026502 (1–10)
8. Pegoraro C, MacNeil S, Battaglia G (2012) Transdermal drug delivery: from micro to nano. Nanoscale 4:1881–1894
9. Kim YC, Park JH, Prausnitz MR (2012) Microneedles for drug and vaccine delivery. Adv Drug Deliv Rev 64:1547–1568
10. DeMuth PC, Min Y, Huang B, Kramer JA, Miller AD, Hammond PT, Irvine DJ (2013) Polymer multilayer tattooing for enhanced DNA vaccination. Nat Mater 12:367–376
11. DeMuth PC, Su X, Samuel RE, Hammond PT, Irvine DJ (2010) Nano-layered microneedles for transcutaneous delivery of polymer nanoparticles and plasmid DNA. Adv Mater 22:4851–4856
12. Strambini LM, Longo A, Diligentia A, Barillaro G (2012) A minimally invasive microchip for transdermal injection/sampling applications. Lab Chip 12:3370–3379
13. Wei Z, Zheng S, Wang R, Bu X, Ma H, Wu Y, Zhu L, Hu Z, Liang Z, Li Z (2014) A flexible microneedle array as low-voltage electroporation electrodes for in vivo DNA and siRNA delivery. Lab Chip 14:4093–4102
14. Pradeep Narayanan S, Raghavan S (2016) Transdermal drug delivery with tiny (micro) needles—an overview. South Asian J Res Eng Sci and Technol 1:378–387
15. Xiang Z, Wang H, Pant A, Pastorin G, Lee C (2013) Development of vertical SU-8 microneedles for transdermal drug delivery by double drawing lithography technology. Biomicrofluidics 7(6): 066501 (1–10)
16. Van der maaden K, Jiskoot W, Bouwstra J (2012) Microneedle technologies for (trans)dermal drug and vaccine delivery. J Control Release 161:645–655
17. Pradeep Narayanan S, Raghavan S (2017) Solid silicon microneedles for drug delivery applications. Int J Adv Manuf Technol 93:407–422
18. Davis SP, Martanto W, Allen MG, Prausnitz MR (2005) Hollow metal microneedles for insulin delivery to diabetic rats. IEEE Trans Biomed Eng 52:909–915
19. Kim K, Lee J-B (2007) High aspect ratio tapered hollow metallic microneedle arrays with microfluidic interconnector. Microsyst Technol 13:231–235
20. Zahn JD, Talbot NH, Liepmann D, Pisano AP (2000) Microfabricated polysilicon microneedles for minimally invasive biomedical devices. Biomed Microdevices 2:295–303
21. Aggarwal P, Johnston CR (2004) Geometrical effects in mechanical characterizing of microneedle for biomedical applications. Sensors Actuators B Chem 102:226–234
22. Wilke N, Mulcahy A, Ye S-R, Morrissey A (2005) Process optimization and characterization of silicon microneedles fabricated by wet etch technology. Microelectron J 36:650–656
23. Tan JL, Tien J, Pirone DM, Gray DS, Bhadriraju K, Chen CS (2003) Cells lying on a bed of microneedles: an approach to isolate mechanical force. Proc Natl Acad Sci U S A 100:1484–1489
24. Arora A, Prausnitz MR, Mitragotri S (2008) Micro-scale devices for transdermal drug delivery. Int J Pharm 364:227–236